Rovibrational Wave-Packet Dispersion during Femtosecond Laser Filamentation in Air

J. H. Odhner, D. A. Romanov, and R. J. Levis

Department of Chemistry and Center for Advanced Photonics Research, Temple University, Philadelphia, Pennsylvania 19122, USA

(Received 21 April 2009; published 14 August 2009)

An impulsive, femtosecond filament-based Raman technique producing high quality Raman spectra over a broad spectral range (1554.7–4155 cm^{-1}) is presented. The temperature of gas phase molecules can be measured by temporally resolving the dispersion of impulsively excited vibrational wave packets. Application to laser-induced filamentation in air reveals that the initial rovibrational temperature is 300 K for both N_2 and O_2. The temperature-dependent wave-packet dynamics are interpreted using an analytic anharmonic oscillator model. The wave packets reveal a $1/e$ dispersion time of 3.9 ps for N_2 and 2.8 ps for O_2. Pulse self-compression of temporal features to 8 fs within the filament is directly measured by impulsive vibrational excitation of H_2.

DOI: 10.1103/PhysRevLett.103.075005 PACS numbers: 52.38.Hb, 33.20.Fb, 78.47.jc

The propagation of femtosecond laser pulses through transparent media results in filamentation when the critical power for self-focusing is exceeded [1–3]. Filamentation is characterized by self-guided propagation over distances larger than the Rayleigh length of the beam, weak plasma formation, and continuum generation. Filamentation sources have been used successfully for light detection and ranging (LIDAR), laser-induced breakdown spectroscopy (LIBS), and fluorescence spectroscopy [4–6]. While the optical processes responsible for continuum generation, pulse self-compression, and generation of high laser intensity have been investigated [1–3], the dynamics of energy partitioning into nuclear coordinates in molecules during filamentation is of interest. The observation of molecular rovibrational dynamics initiated by optical filamentation [7] demonstrates the coherent nature of the excitation generated by a filament and suggests the use of filaments for nonlinear vibrational spectroscopy. The interaction of two filaments through rotational quantum wakes [8] dominates propagation effects.

The process of femtosecond filamentation leads to the generation of very short laser pulses, approaching the single cycle regime. Prediction [9] and postfilament characterization [10] of pulse compression through filamentation, without additional chirp-compensation, to pulse durations of <8 fs have been performed. This pulse duration is sufficiently short to impulsively excite any vibrations in a medium coherently. Indeed, excitation of vibrations up to 4158.6 cm^{-1} has been confirmed by the recent measurement of the impulsively excited fundamental vibrational mode of H_2 in a filament using 10 fs driving pulses [7]. Here we show that the temporal dynamics of molecular vibrations in the filament wake can be used to measure the energy partitioning during the excitation process. We report the measurement of the vibrational dispersion time of N_2 and O_2 after impulsive excitation using filament-based femtosecond stimulated Raman spectroscopy. The dispersion time of the prepared rovibrational wave packet reveals that the initial rovibrational temperature of the filament is near 300 K. In addition, we observe self-compression within the plasma channel of a filament through measurement of vibrational features corresponding to periods as short as 8 fs.

In this experiment, a 2.5 mJ, 45 fs, 1 kHz, 800 nm laser is used to create a filament pump pulse (2 mJ) and a 400 nm probe pulse (1.65 μJ, 1.5 ps, 30 cm^{-1} FWHM bandwidth). The probe pulse is generated by filtering (3 nm FWHM) the fundamental, rotating the polarization with a half-wave plate, and frequency doubling in a 6 mm β-barium borate (BBO) crystal, which further narrows the spectrum. Alternatively, a 1 mm BBO crystal can be used without the spectral filter for improved temporal resolution. The probe pulse passes through an optical delay line and is focused using an $f = 50$ cm lens at a small angle ($\theta = 1.5°$) with respect to the filament, as shown in Fig. 1. The filament is generated by focusing the 2 mJ pump into atmospheric air with a 2 m lens. The 2 m lens is placed on a 30 cm-long translation stage and the spatial overlap of the filament and the 400 nm beam is optimized for maximum coherent excitation in air. Filamentation of the pump pulse is inferred by the extended ($\sim$30–50 cm) visible fluorescence (plasma) channel in air, and the clean spatial mode and white light observed after the filament. The interaction region is preceded by an open-ended one-inch diameter, 30 cm-long tube to reduce turbulence.

The Raman signal travels nearly collinearly with the 400 nm probe beam, and the spectrum is measured after spatially filtering the probe in the Fourier plane of a reflective 4-f spectrometer formed by a prism and a cylindrical mirror ($f = 30$ cm). Both the Stokes and anti-Stokes lines were observable with comparable intensity and exhibited similar temporal dynamics. For simplicity we present only the Stokes measurements here. For single-shot measurements of the vibrational spectrum, a positive delay (pump preceding probe) of 1–1.5 ps is introduced between the pump and the probe to avoid cross-phase modulation of the probe pulse.

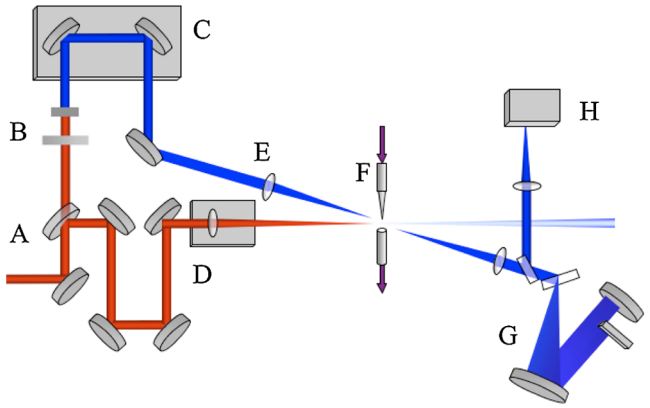

FIG. 1 (color online). The experimental setup for filament-based stimulated Raman scattering. (a) beam splitter, (b) half–wave plate, filter, and 6 mm BBO crystal, (c) delay stage, (d) 2 m lens, (e) 0.5 m lens, (f) air flow and low vacuum to stabilize interaction region, (g) Fourier filter to remove pump, and (h) spectrometer (USB2000, 175–500 nm). To reduce air turbulence a one-inch diameter, 30 cm-long open-ended tube precedes the overlap region (not shown).

The filament-based femtosecond stimulated Raman spectrum for air is shown in Fig. 2. The Raman spectrum is background free due to the noncollinear geometry of our experimental setup. The Raman lines of oxygen and nitrogen (1554.7 and 2330.7 cm^{-1}, respectively) are detected with spectral resolution dictated by the convolution of the probe pulse bandwidth (30 cm^{-1}) and the spectrometer resolution (18 cm^{-1} at 400 nm). The ratio of the nitrogen/oxygen Raman peaks, ~15:1, is consistent with the ~17:1 ratio calculated using Raman gain coefficients and atmospheric concentrations. We assume uniform excitation of the sample in the interaction region. Theoretical and experimental evidence of asymmetric pulse profiles and pulse splitting during and after filamentation (see [1–3], and references therein) suggest that this assumption is only valid to a first approximation, and that the pulse duration depends strongly on input parameters and probe position along the filament length. The spectrum was recorded at a positive delay, where there is no temporal overlap between the pulses. The lack of temporal overlap indicates impulsive excitation within the filament and shows that the response is not a result of spectral overlap between appropriately spaced spectral components of the pump and probe beams. This implies self-compression of the filament excitation pulse to less than 14.3 fs (the vibrational period of nitrogen) in ambient air, and supports our assumption of uniform impulsive excitation. This excitation mechanism is consistent with other four-wave mixing spectroscopic techniques such as CARS [11].

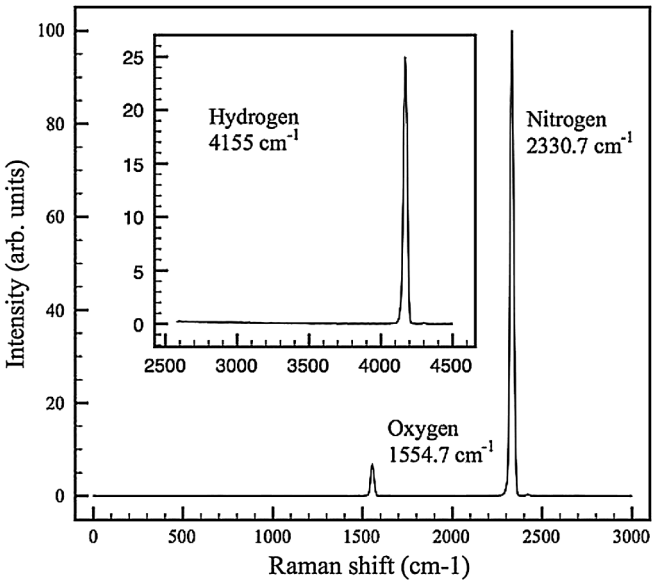

FIG. 2. The vibrational Raman spectrum of air. The sample was impulsively excited using a filament and probed using a 1.5 ps, 400 nm pump beam. Inset: the vibrational Raman spectrum of H_2 taken using the same setup.

The impulsive nature of the vibrational excitation in a filament can be investigated by measuring the Raman response as a function of time delay between the filament pump and the 400 nm probe. The time dependence of the N_2 and O_2 vibrational response is shown in Fig. 3. At zero delay between the pump and probe beams, cross-phase modulation of the probe pulse can be observed in the oxygen signal, but is not present in the nitrogen signal because spectral broadening of the probe does not extend to this region. Longer pump-probe delay times (5–20 ps) result in diminishing intensity of both the N_2 and O_2 Raman lines. The time required for the signal to drop by a factor of $1/e$ is 3.9 ps for N_2 and 2.8 ps for O_2. As will be seen, this can be attributed to the dispersion of the vibrational coherence due to excitation of a superposition of rovibrational states.

During impulsive excitation, all thermally populated rovibrational states of nitrogen and oxygen having vibra-

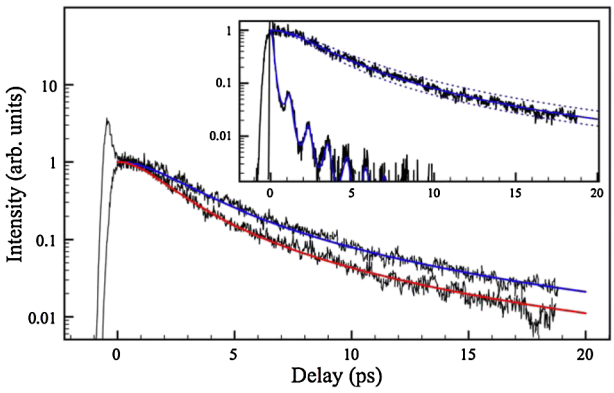

FIG. 3 (color online). Time dependence of the normalized Raman signal for N_2 and O_2. The theoretical fits for both are for 300 K. Inset: A comparison of experimental measurements of N_2 in air and N_2 in a methane flame with theoretical model from Eq. (3) for 300 and 3000 K, respectively. The dashed lines (inset) show calculations for N_2 decay with temperatures of 300 ± 50 K.

tional periods longer than the pulse duration or temporal substructure contained in the pulse are excited. Filamentation results from a dynamic interplay between several nonlinear effects, including self-steepening, space-time focusing, group-velocity dispersion, and plasma generation, which collectively result in a short pulse that impulsively drives the Raman response. A coherent rovibrational Raman transition will occur whenever two frequencies with spacing ΔE equal to a rovibrational transition arrive simultaneously in the sample. Subsequent interference between the coherent vibration and the macroscopic polarization imposed on the medium by the picosecond Raman probe generates Raman sidebands. Experiments in a hollow waveguide [12] suggest that self-steepening is the driving mechanism for impulsive vibrational excitation of N_2 and CO_2. To test this hypothesis, we can investigate Raman generation at a laser intensity smaller than the critical power for filamentation, thus precluding broad bandwidth generation, self-compression, and self-steepening [1–3]. At intensities below the critical power, diffraction effects exceed Kerr lensing and no filamentation occurs. The critical power for filamentation is given by $P_{\mathrm{crit}} = 3.77\lambda_0{}^2/8\pi n_0 n_2$, where λ is the laser wavelength, n_0 is the index of refraction, and n_2 is the second order, intensity dependent index of refraction for the material. In air, at standard temperature and pressure the critical power is 3.2 GW [13]; below this value no detectable Raman gain is observed.

The time dependence of the Raman response of a sample is a function of the rovibrational structure of the constituent molecules and the temperature of the system. The time dependence can be used to study the dynamics in a medium after excitation, in this case caused by filamentation, and thus can be used to determine energy partitioning into vibrational modes during the filamentation process. The initial thermal population defines the coherent superposition of excited rovibrational states, which in turn determines the temporal propagation of the wave packet. As pointed out previously [14], the vibrations of the excited rovibrational states will initially be in phase, but will destructively interfere as time proceeds (dispersion) due to the differences in spacing between rovibrational energy levels in an anharmonic potential well. The dispersion of rovibrational coherence in the sample is manifested as a decrease in the signal intensity as a function of pump-probe time delay. Collinear pump-probe measurements show that the rotational response dominates the vibrational Raman spectrum at times corresponding to fractional rotational revivals (not shown). This response is suppressed in the noncollinear measurements because far less nonlinear phase is accumulated.

The two major causes for the dispersion of the wave packet are the anharmonicity of the molecular potential energy surface and the rotation-vibration coupling. The former reduces vibrational level spacing with increasing n, and the latter decreases the rovibrational level spacing with increasing n, as shown in Fig. 4. The short duration of the filament pulse leads to excitation of all thermally populated states, which leads to dispersion if the oscillators have different frequencies due to anharmonicity and/or rotation-vibration coupling. We test this hypothesis by comparing the observed decay with that predicted by a simple model that includes first-order corrections for anharmonicity and rotation-vibration coupling, $E_{n,J} = \hbar\omega_e(n + 1/2) - \hbar\omega_e x_e(n + 1/2)^2 + (B_e - \alpha_e n)J(J + 1)$, where ω_e is the vibrational mode frequency, $\omega_e x_e$ is the anharmonicity parameter, B_e is the rotational constant, and α_e is the rotation-vibration coupling parameter. Restricting ourselves to the Q branch, the impulsive Raman excitation of the system induces all possible interlevel transitions with $\Delta n = 1$ and $\Delta J = 1$, thus creating a time-dependent polarization of the medium whose evolution is determined by oscillations at frequencies, $\omega_{n,J} = \omega_e - 2\omega_e x_e(n + 1) - (\alpha_e/\hbar)J(J + 1)$:

$$P(t) = \sum_{n,J} A_{n,J}(T)\cos[\omega_{n,J}t] = \mathrm{Re}\left\{\sum_{n,J} A_{n,J}(T)\exp[i\omega_{n,J}t]\right\}, \quad (1)$$

where the temperature-dependent amplitudes, $A_{n,J}(T)$, are determined by the initial thermal-equilibrium populations of the Jth sublevel of nth vibrational manifold. Over a wide range of temperatures, the double inequality, $B_e \ll kT \ll \hbar\omega_e$, holds, which allows effective decoupling of the summations over n and over J, extending the upper limit of the n sum to infinity and replacing the J sum with an integral. Actually, at room temperature, there is very little population above the ground-vibrational-state manifold and within this manifold the rotations to approximately $J = 20$ are populated [15]. In this limit, the polarization emerges as oscillations with the frequency ω_e, modified

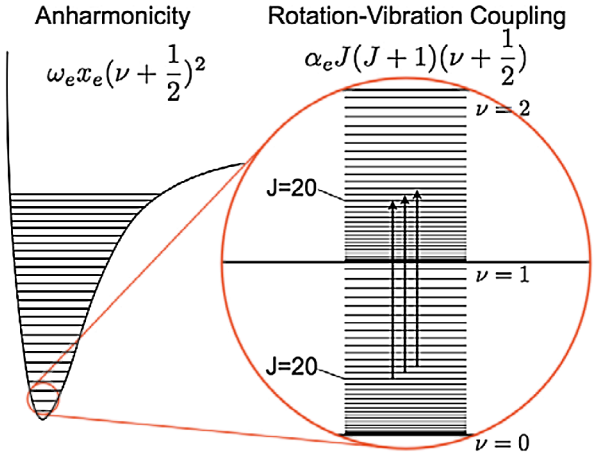

FIG. 4 (color online). A schematic of the two main sources of dispersion of the molecular wave packet; anharmonicity and rotation-vibration coupling. The change in oscillator frequency due to these corrections results in the time-dependent dispersion modeled in Eq. (3).

by the temperature-dependent envelope

$$P(t) \sim \mathrm{Re}\left\{\frac{\exp[it(\omega_e - 2\omega_e x_e)][2\exp(\frac{2B_e}{kT}) + \exp(-i\frac{2\alpha_e}{\hbar}t)]}{(\frac{2B_e}{kT} + i\frac{2\alpha_e}{\hbar}t)[\exp(\frac{\hbar\omega_e}{kT}) - \exp(-2i\omega_e x_e t)]}\right\}. \quad (2)$$

Upon interaction with the probe pulse of duration $\sigma \gg 1/\omega_e$, these polarization oscillations result in a Raman signal whose intensity depends on the pump-probe time-delay, t_d. In particular, the evolution of the Stokes signal intensity is found as

$$I_S(t_d) \sim \frac{[\exp(\frac{2B_e}{kT}) + \frac{1}{2}]^2 - \sin^2(\frac{\alpha_e}{\hbar}t_d)}{[1 + (\frac{\alpha_e T}{B_e \hbar}t_d)^2][\sinh^2(\frac{\hbar\omega_e}{2kT}) + \sin^2(\omega_e x_e t_d)]}. \quad (3)$$

The signal decay is mainly determined by the first factor in the denominator, arising from rotation-vibration coupling. The vibrational anharmonicity is found in the second factor in the denominator and results in oscillatory modulation of the signal with the characteristic frequency, $2\omega_e x_e$. At room temperature the modulation depth $[\sinh(\hbar\omega_e/2kT)]^{-2}$ is limited to $\sim$1%, and will be more pronounced at elevated temperatures.

The intensity $I_S(t)$ is plotted in Fig. 3 for nitrogen and oxygen at 300 K. This temperature fits the data well, suggesting that the room temperature air acquires very little vibrational excitation during the filamentation process. This is reasonable, given that the time required for plasma electrons to transfer energy to vibrational modes is much longer than the measured ps dispersion time. The 3.9 ps dispersion time for N_2 is also in good agreement with previous CARS measurements at room temperature [14], where a full quantum treatment was used to model the measurements. The agreement between the CARS and impulsive Raman measurements suggests that the temperature of a gas can be measured using this two beam spectroscopic method. Our measurements reveal a dispersion time of 2.8 ps for oxygen, which is shorter than that measured for N_2. The difference in dispersion time between N_2 and O_2 reflects the difference in the rovibrational structure of the two molecules. Note that the O_2 measurement also is fit well using a temperature of 300 K.

To test the utility of the heterodyned, impulsive filament-based, stimulated Raman spectroscopy method as a means to determine temperature, we measured the decay of the N_2 signal in a methane flame above a flat burner. The dispersion measurement is shown in the inset to Fig. 3. The Stokes signal intensity $I_S(t)$ is plotted for a temperature of 3000 K, which is reasonable given that the adiabatic temperature of a methane-oxygen flame is 2916 K. The model reproduces the modulations observed at high temperatures as well.

The noncollinear method provides a direct measurement of the evolution of temporal structure of the pulse envelope in the filament plasma channel. The highest frequency vibration that we have measured is that of hydrogen, with a vibrational period $\sim$8 fs, corresponding to 4158.6 cm^{-1}, shown in the inset of Fig. 2. As such, this data cannot be construed as a direct measurement of the pulse duration, as impulsive excitation requires only the substructure of the pulse to be shorter than the vibrational period [12]. However, this measurement is still useful for characterizing the evolution of temporally short structures in the plasma channel. Simulations suggest that the duration of the temporal features in the filament change nonmonotonically with position and that single-cycle temporal features may be formed [16].

Measurement of the rovibrational dispersion time of an impulsively excited wave packet can be used to determine the rovibrational temperature in a filament. For a filament formed with a 2 mJ, 800 nm, 60 fs laser pulse, we find that the initial rovibrational temperature is 300 K. We conclude that no energy is initially partitioned into molecular vibrations in the ground electronic state as a result of strong field excitation during the filamentation process. Time-dependent measurements in microplasmas reveal that the electronic temperature decreases on a time scale of hundreds of picoseconds, which may result in subsequent vibrational excitation at time scales longer than those measured here [17]. The self-compression of a pulse undergoing filamentation in air is directly measured by performing heterodyned, impulsive, filament-based stimulated Raman spectroscopy on N_2, O_2, and H_2 in the plasma channel. Our measurements demonstrate self-compressed temporal features at least as short as 8 fs in air.

We would like to thank Mateusz Plewicki for useful discussions. This work was supported by the National Science Foundation (Grant No. CHE0518497) and the Army Research Office (Grant No. W911NF0810020).

[1] L. Berge *et al.*, Rep. Prog. Phys. **70**, 1633 (2007).
[2] S. Chin *et al.*, Can. J. Phys. **83**, 863 (2005).
[3] A. Couairon and A. Mysyrowicz, Phys. Rep. **441**, 47 (2007).
[4] J. F. Daigle *et al.*, Appl. Phys. B **93**, 759 (2008).
[5] P. Rairoux *et al.*, Appl. Phys. B **71**, 573 (2000).
[6] K. Stelmaszczyk *et al.*, Appl. Phys. Lett. **85**, 3977 (2004).
[7] F. Calegari *et al.*, Opt. Lett. **33**, 2922 (2008).
[8] Y. H. Chen, S. Varma, and H. M. Milchberg, J. Opt. Soc. Am. B **25**, B122 (2008).
[9] O. G. Kosareva *et al.*, Laser Phys. Lett. **4**, 126 (2007).
[10] G. Stibenz, N. Zhavoronkov, and G. Steinmeyer, Opt. Lett. **31**, 274 (2006).
[11] R. W. Boyd, *Nonlinear Optics* (Academic Press, San Diego, CA, 2003), p. 576.
[12] R. A. Bartels *et al.*, Chem. Phys. Lett. **374**, 326 (2003).
[13] S. Akturk *et al.*, Opt. Express **15**, 15260 (2007).
[14] R. P. Lucht *et al.*, Appl. Phys. Lett. **89**, 251112 (2006).
[15] S. Varma, Y. H. Chen, and H. M. Milchberg, Phys. Rev. Lett. **101**, 205001 (2008).
[16] A. Couairon *et al.*, J. Mod. Opt. **53**, 75 (2006).
[17] A. Filin *et al.*, Phys. Rev. Lett. **102**, 155004 (2009).